

Magnetic field dependence of the coupling efficiency of a superconducting transmission line due to the proximity effect

S. Zhu, T. Zijlstra, A. A. Golubov, M. van den Bemt, A. M. Baryshev, and T. M. Klapwijk

Citation: [Applied Physics Letters](#) **95**, 253502 (2009); doi: 10.1063/1.3276076

View online: <http://dx.doi.org/10.1063/1.3276076>

View Table of Contents: <http://scitation.aip.org/content/aip/journal/apl/95/25?ver=pdfcov>

Published by the [AIP Publishing](#)

Articles you may be interested in

[Quantum dot spectroscopy of proximity-induced superconductivity in a two-dimensional electron gas](#)
Appl. Phys. Lett. **98**, 132101 (2011); 10.1063/1.3570660

[Proximity effect and interface transparency in Nb/Cu multilayers](#)
J. Appl. Phys. **106**, 113917 (2009); 10.1063/1.3267868

[Planar S-\(S/F\)-S Josephson junctions induced by the inverse proximity effect](#)
Appl. Phys. Lett. **95**, 062501 (2009); 10.1063/1.3200226

[Magnetism and superconductivity in the superconductor/quasimagnet/ferromagnet Nb Pd Fe system](#)
J. Appl. Phys. **103**, 07C703 (2008); 10.1063/1.2829237

[Direct Observation Of The Proximity Effect In The N Layer In A MultiTerminal SINIS Josephson Junction](#)
AIP Conf. Proc. **850**, 983 (2006); 10.1063/1.2355035



Magnetic field dependence of the coupling efficiency of a superconducting transmission line due to the proximity effect

S. Zhu,^{1,a)} T. Zijlstra,¹ A. A. Golubov,² M. van den Bernt,³ A. M. Baryshev,³ and T. M. Klapwijk¹

¹Faculty of Applied Sciences, Kavli Institute of Nanoscience, Delft University of Technology, Lorentzweg 1, 2611 CJ Delft, The Netherlands

²Faculty of Science and Technology and MESA, Institute of Nanotechnology, University of Twente, 7500 AE Enschede, The Netherlands

³SRON National Institute for Space Research, Landleven 12, 9747 AD Groningen, The Netherlands

(Received 23 September 2009; accepted 29 November 2009; published online 22 December 2009)

The coupling efficiency of a Nb superconducting transmission line has been measured using a Fourier transform spectrometer for different magnetic fields. It is found that the coupling decreases with increasing magnetic field when the frequency is close to the gap of the Nb superconductor. This is attributed to the changes of the surface impedance of the proximity-coupled superconductor/normal-metal bilayers in the transmission line. © 2009 American Institute of Physics.

[doi:10.1063/1.3276076]

The surface of a superconducting film plays a very important role in the low temperature properties of superconducting devices, in providing magnetic moments, a dielectric surface layer, or a poorly superconducting layer with depressed gap.¹⁻³ This raises the question to what extent the electrodynamic properties of a superconducting film (S) are influenced by a thin normal metal (N). Surface impedance measurements on a Nb/Al bilayer have shown that there is no difference between a Nb/Al bilayer and a Nb bare layer at GHz frequencies if the Al thickness is less than 10 nm.⁴ However, our recent measurements have shown evidence that close to THz frequencies the surface impedance of a Nb/Al bilayer with Al thickness down to 6 nm is influenced by the thin N layer.⁵ The experiment was triggered by the introduction of high-current density AlN-barrier junctions for Atacama Large Millimeter Array.⁶ Because of their smaller areas higher magnetic fields are needed, which lead to a deterioration of the performance of the superconductor-insulator-superconductor (SIS) quasiparticle mixer. Here we demonstrate the effects of a S/N bilayer on the coupling efficiency of a Nb superconducting transmission line (TL), using a SIS tunnel junction as a direct detector. The results are analyzed in terms of the proximity effect theory.

The Nb-based TL and SIS junction have been fabricated using the sputtering technology.⁷ Fig. 1 illustrates the cross-section and the equivalent circuit of the TL and the junction. The TL is used to couple the rf radiation to the junction. The radiation is collected by a horn antenna with a waveguide, picked up at the probe point, and transmitted to the junction via the TL. The antenna and waveguide are modeled as the source impedance Z_{ant} , determined by the structure of the horn and waveguide, the mounting position, and the substrate thickness.⁸ The junction is characterized by the normal state resistance R_n and the geometric capacitance C_j [with junction impedance $Z_j = R_n / (1 + j\omega R_n C_j)$]. The TL is represented as the inductance L and the impedance transformer Z_{tran} , which are used to tune out C_j and provide the match between Z_{ant} and Z_j . The radiation coupling is evaluated with

a Fourier transform spectrometer (FTS) measurement performed with a Michelson interferometer.⁹ The measured interferogram is the modulation of the junction current induced by the broadband radiation source as a function of the position of the movable mirror. The Josephson current is suppressed by a magnetic field generated by a superconducting coil (coil current I_m) connected to the soft iron pole shoes.

The dc I - V measurements (Fig. 2) are used to determine the value of $R_n (=18 \Omega)$, which with the known value of $R_n A$ -product determined from a $2 \times 2 \mu\text{m}^2$ junction gives the area of the junction ($A = 0.4 \mu\text{m}^2$). The specific capacitance $C_s (=C_j/A)$ is assumed to be $60 \text{ fF}/\mu\text{m}^2$.⁶ Normally, it is assumed that the magnetic field needed to suppress the Josephson current does not affect the sharp nonlinearity at the gap and also not the TL properties. However, with the present generation of high-current density junctions⁷ the junction areas have become smaller to match the impedance and therefore higher magnetic fields are needed to suppress the Josephson-currents.

The inset of Fig. 3 shows the full FTS response at $I_m = 6.0 \text{ mA}$ (about 0.022 Tesla as derived from the Fraunhofer pattern for the diamond-shaped junction). The TL is designed

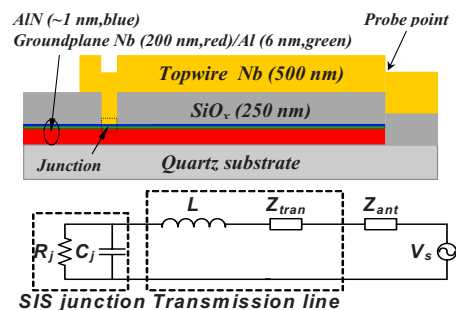


FIG. 1. (Color online) Upper: schematic cross-section of the TL and SIS junction. The rf radiation is collected by a horn with a waveguide (not shown here) and picked up at the probe point. The Nb/Al groundplane forms the proximity coupled bilayer. The Nb topwire on amorphous SiO_x layer has nonuniform properties (see Ref. 8) turning it effectively into a bilayer. Lower: equivalent circuit of the TL with the junction, as well as the antenna and waveguide.

^{a)}Electronic mail: s.zhu@tudelft.nl.

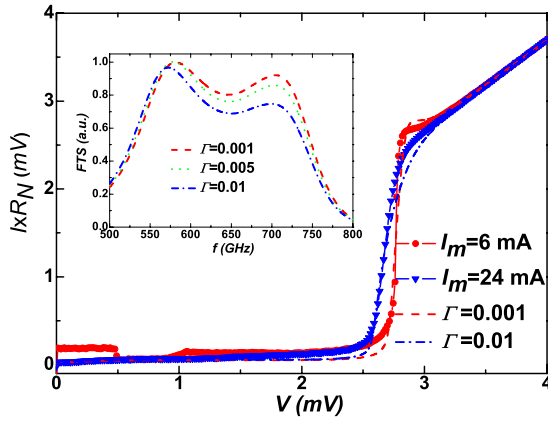


FIG. 2. (Color online) Typically measured (symbols+lines) and calculated (lines) I - V curves of the junction at 4.2 K. A Dynes broadening parameter (Ref. 16) of $10 \mu\text{eV}$ is used for the top Nb electrode. The Josephson current is not included in the fitting. Inset: theoretical predictions of FTS response when only considering the influence of Nb/Al ground plane.

to obtain the maximum FTS response between 600 and 720 GHz.⁶ The minima in the curves at 560 and 750 GHz are due to water absorption occurring in the optical path. In order to compare the FTS measurements with model calculations, we subtract the atmospheric absorption from the data with an estimated transmission of 60%.¹⁰ When the magnetic field is applied, the FTS decreases monotonically between 630 and 730 GHz with a stronger effect at the upper side of the band (the gap frequency of Nb is $f_{\text{gap}} \sim 680$ GHz).

The coupling efficiency of the TL is calculated from $\eta_{\text{rf}} = 1 - |(Z_m - Z_{\text{ant}}^*) / (Z_m + Z_{\text{ant}}^*)|^2$, where Z_m is the impedance combination of TL and junction. The characteristic impedance of TL is given by $Z_0 = \sqrt{Z/Y}$, where $Y = j\omega\epsilon_r\epsilon_0/d$ and $Z = j2\pi f\mu_0 d/w + (Z_{s1} + Z_{s2})/w$ are the shunt admittance and series impedance, with $\epsilon_r (=3.8)$ the permittivity, d the thickness of the SiO_x layer, and w the width of topwire. Z_{s1} and Z_{s2} are the surface impedances of superconducting topwire and ground plane of the TL. Since the magnetic field has no influence on the junction (R_n and C_j) and the SiO_x layer, the magnetic field dependence of the FTS response should be determined by Z_{s1} and Z_{s2} of the TL.

The surface impedance of a dirty superconductor with finite thickness d is expressed as¹¹ Z_s

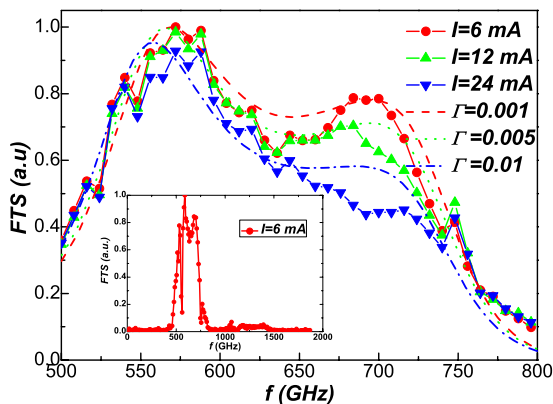


FIG. 3. (Color online) Measured (symbols+lines) and calculated (lines) FTS responses of the TL at 4.2 K, both of which are normalized to the maximum value of the curve at $I=6$ mA and $\Gamma=0.001$, respectively. The atmospheric absorption has been removed from the measured data. The inset shows the full FTS response at $I_m=6$ mA.

$= \sqrt{j\omega\mu_0/\sigma} \coth(d\sqrt{j\omega\mu_0\sigma})$, where $\sigma (= \sigma_1 - j\sigma_2)$ is the complex conductivity of the superconductor, which is determined from Nam's expressions¹²

$$\frac{\sigma_1}{\sigma_N} = \frac{1}{\hbar\omega} \left\{ \int_{\Delta-\hbar\omega}^{-\Delta} g_1(1,2) \tanh\left(\frac{\hbar\omega + \epsilon}{2k_B T}\right) d\epsilon + \int_{\Delta}^{\infty} g_1(1,2) \times \left[\tanh\left(\frac{\hbar\omega + \epsilon}{2k_B T}\right) - \tanh\left(\frac{\epsilon}{2k_B T}\right) \right] d\epsilon \right\}, \quad (1a)$$

$$\frac{\sigma_2}{\sigma_N} = \frac{1}{\hbar\omega} \left\{ \int_{\Delta-\hbar\omega}^{\Delta} g_2(1,2) \tanh\left(\frac{\hbar\omega + \epsilon}{2k_B T}\right) d\epsilon + \int_{\Delta}^{\infty} \left[g_2(1,2) \tanh\left(\frac{\hbar\omega + \epsilon}{2k_B T}\right) + g_2(2,1) \tanh\left(\frac{\epsilon}{2k_B T}\right) \right] d\epsilon \right\}. \quad (1b)$$

Here the coherence factors $g_{1,2}$ are given by

$$g_1(1,2) = \text{Re}[N(1)]\text{Re}[N(2)] + \text{Re}[P(1)]\text{Re}[P(2)], \quad (2a)$$

$$g_2(1,2) = \text{Im}[N(1)]\text{Re}[N(2)] + \text{Im}[P(1)]\text{Re}[P(2)], \quad (2b)$$

where $N(=\cos \theta)$ and $P(=\sin \theta)$ are generalized densities of states (DOS) of the superconductor. θ is a measure of the strength of superconducting state. The arguments 1 and 2 represent the quasiparticle energy ϵ and $\epsilon + \hbar\omega$.

The proximity-effect of the S/N bilayer can be described by the Usadel equations for the parameter θ (Ref. 13)

$$\xi_{S,N}^{*2} \frac{\partial^2}{\partial x^2} \theta_{S,N} + j\epsilon \sin \theta_{S,N} + \Delta_{S,N} \cos \theta_{S,N} = 0, \quad (3a)$$

$$\Delta_{S,N} \ln \frac{T}{T_{c,S}} + 2 \frac{T}{T_{c,S} \omega_n} \sum \left(\frac{\Delta_{S,N}}{\omega_n} - \sin \theta_{S,N} \right) = 0, \quad (3b)$$

with boundary conditions at the S-N interface

$$\xi_S^* \frac{\partial}{\partial x} \theta_S(0) = \gamma \xi_N^* \frac{\partial}{\partial x} \theta_N(0), \quad \gamma = \frac{\rho_S \xi_S^*}{\rho_N \xi_N^*}, \quad (4a)$$

$$\sin[\theta_S(0) - \theta_N(0)] = \gamma_B \xi_N^* \frac{\partial}{\partial x} \theta_N(0), \quad \gamma_B = \frac{R_B}{\rho_N \xi_N^*}, \quad (4b)$$

and at the free surfaces $\frac{\partial}{\partial x} \theta(x) = 0$ ($x = -d_N$ and d_S). The parameter θ is a function of the position x and quasiparticle energy ϵ . ξ^* is the effective coherence length defined as $\xi_{S,N}^* = \sqrt{\hbar D_{S,N} / 2\pi k_B T_{c,S}}$ ($D = l_e v_F / 3$ the diffusion coefficient, l_e the mean-free path and v_F the Fermi velocity). γ and γ_B are the interface parameters to be determined. Details of other parameters can be found in Ref. 13. The quasiparticle DOS is defined as $n(\epsilon) = \text{Re}[\cos \theta]$. When a weak magnetic field is applied, the quasiparticle energy is changed to $\epsilon + j\Gamma \cos[\theta(x)]$. Here, $\Gamma = (H \xi_S^* W / \Phi_0)^2 \pi^{1/3}$ is the effective pair-breaking rate, in which H is the magnetic field, W the thickness of the bilayer, and Φ_0 the flux quantum.¹⁴

From Eq. (4a), γ can be determined if either ρ or l_e is known. For the thin Al layer l_e is assumed to be equal to the film thickness. Using the parameters listed in Table I, γ is found to be 0.35 for the Nb/Al bilayer. Based on a fit to the I - V curve (for $I_m = 6$ mA) around the gap voltage, γ_B is set as

TABLE I. Parameters of Al and Nb films. Nb films are deposited on the amorphous SiO_x layer. ρ and l_e are interrelated by the intrinsic value of $\rho \cdot l_e$.

	d (nm)	T_c (K)	$\rho \cdot l_e$ ($\mu\Omega \text{ cm}^2$)	ρ ($\mu\Omega \text{ cm}$)	l_e (nm)	v_F (m s^{-1})	ξ^* (nm)
Al	6	1.3	4.0×10^{-6}	6.7	6.0	1.34×10^6	18.7
Nb	200	9.25	3.7×10^{-6}	4.2	8.8	0.28×10^6	10.4
Nb*	20	7.5	3.7×10^{-6}	10.0	3.7	0.28×10^6	6.8

1.0 (consistent with Ref. 15). The pair-breaking rate Γ is determined from the I - V curves for finite I_m values (Fig. 2) and the same values of Γ are used to fit the FTS response shown in Fig. 3. By solving Eqs. (1) and (3), DOS and σ of the Nb/Al bilayer are determined (Fig. 4). In order to calculate Z_s of the bilayer we take the value of σ at $x = -d_N$ and assume the same value over the whole thickness of the bilayer. The Nb topwire is initially treated as a normal BCS superconductor with $V_g = 2.8$ mV and $\rho = 4.2 \mu\Omega \text{ cm}^2$. The predicted FTS responses are shown in the inset of Fig. 2. They show the trend in the direction observed in the experiments (Fig. 3) but with a weaker dependence.

This led us to further consider the film quality of the 500 nm Nb topwire on the amorphous SiO_x layer. Independent measurements have shown that both T_c and σ_N of the Nb film with thickness less than 20 nm decrease.⁸ Therefore, we use the additional conjecture that the Nb topwire forms a proximity bilayer consisting of Nb(480 nm)/Nb* (20 nm) bilayer. Using the measured data on 20 nm Nb film, γ is calculated to be 0.64 and γ_B is simply taken as 1.0. The procedures of the calculation are the same as the ones for the Nb/Al bilayer.

Using the calculated Z_s of both Nb/Al and Nb/Nb* bilayers, the FTS responses of the TL are calculated. The re-

sults are shown in Fig. 3. It is seen that the measurements can be well understood by this theoretical analysis. We conclude that the observed decrease of the coupling around f_{gap} is due to the increase of Z_s of the inhomogeneous Nb topwire and the Nb/Al ground plane. The results demonstrate that at high frequencies the proximitised superconducting properties are deteriorated by the application of a magnetic field. An obvious solution at these frequencies is to avoid the use of bilayers.¹⁷

We thank R. Barends, C. F. J. Lodewijk, N. Verbruggen, and A. Brettschneider for helpful discussions. This work was supported in part by NanoImpuls, the Dutch Research School for Astronomy (NOVA), the Dutch Organization for Scientific Research (NWO), Radionet, and the European Southern Observatory (ESO).

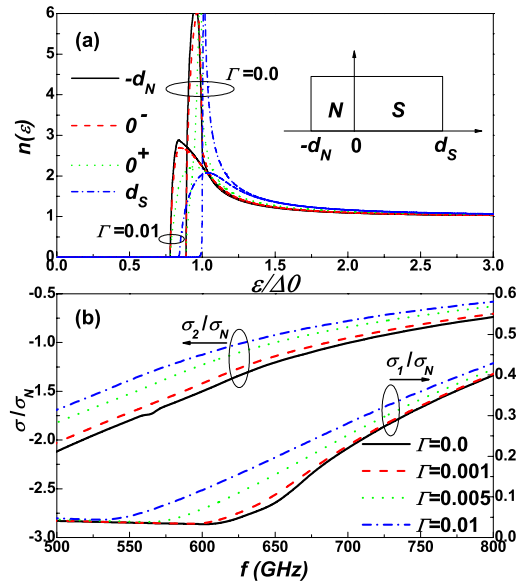


FIG. 4. (Color online) (a) DOS at the surfaces and interfaces of the Nb/Al bilayer. Δ_0 is the calculated gap energy of bulk Nb. (b) Complex conductivities σ/σ_N at the surface of Al layer ($x = -d_N$).

¹R. H. Koch, D. P. DiVincenzo, and J. Clarke, *Phys. Rev. Lett.* **98**, 267003 (2007).

²R. Barends, H. L. Hortensius, T. Zijlstra, J. J. A. Baselmans, S. J. C. Yates, J. R. Gao, and T. M. Klapwijk, *Appl. Phys. Lett.* **92**, 223502 (2008).

³G. B. Arnold, J. Zasadzinski, and E. L. Wolf, *Phys. Lett. A* **69**, 136 (1978).

⁴M. S. Pambianchi, S. N. Mao, and S. M. Anlage, *Phys. Rev. B* **52**, 4477 (1995).

⁵S. Zhu, T. Zijlstra, C. F. J. Lodewijk, A. Brettschneider, M. van den Bemt, B. D. Jackson, A. M. Baryshev, A. A. Golubov, and T. M. Klapwijk, Proceedings of the 20th International Symposium on Space THz Tech. Charlottesville, VA, 2009, pp. 271–274.

⁶C. F. J. Lodewijk, T. Zijlstra, S. Zhu, F. P. Mena, A. M. Baryshev, and T. M. Klapwijk, *IEEE Trans. Appl. Supercond.* **19**, 395 (2009).

⁷T. Zijlstra, C. F. J. Lodewijk, N. Verbruggen, F. D. Tichelaar, D. N. Loudkov, and T. M. Klapwijk, *Appl. Phys. Lett.* **91**, 233102 (2007).

⁸C. F. J. Lodewijk, O. Noroozian, D. N. Loudkov, T. Zijlstra, A. M. Baryshev, F. P. Mena, and T. M. Klapwijk, *IEEE Trans. Appl. Supercond.* **17**, 375 (2007).

⁹G. de Lange, J. J. Kuipers, T. M. Klapwijk, R. A. Panhuyzen, H. van de Stadt, and M. W. M. de Graauw, *J. Appl. Phys.* **77**, 1795 (1995).

¹⁰The program that calculates the atmospheric transmission has been provided by J. R. Pardo-Carrion, Departamento de Astrofísica Molecular e Infrarroja, Consejo Superior de Investigaciones Científicas, Madrid, Spain.

¹¹R. L. Kautz, *J. Appl. Phys.* **49**, 308 (1978).

¹²S. B. Nam, *Phys. Rev.* **156**, 470 (1967).

¹³A. A. Golubov, E. P. Houwman, J. G. Gijsbertsen, V. M. Krasnov, J. Flokstra, H. Rogalla, and M. Yu. Kupriyanov, *Phys. Rev. B* **51**, 1073 (1995).

¹⁴W. Belzig, C. Bruder, and G. Schön, *Phys. Rev. B* **54**, 9443 (1996).

¹⁵A. Zehnder, Ph. Lerch, S. P. Zhao, Th. Nussbaumer, E. C. Kirk, and H. R. Ott, *Phys. Rev. B* **59**, 8875 (1999).

¹⁶R. C. Dynes, V. Narayanamurti, and J. P. Garno, *Phys. Rev. Lett.* **41**, 1509 (1978).

¹⁷B. D. Jackson, A. M. Baryshev, G. de Lange, J. R. Gao, S. V. Shitov, N. N. Iosad, and T. M. Klapwijk, *Appl. Phys. Lett.* **79**, 436 (2001).